Fast 1D inversion of towed streamer electromagnetic data to estimate vertical and horizontal resistivity

Johan Mattsson* and Folke Engelmark, PGS

This paper was prepared for presentation during the 13th International Congress of the Brazilian Geophysical Society held in Rio de Janeiro, Brazil, August 26-29, 2013.

Abstract

The Alvheim – Boa Field located in the North Sea was surveyed in October 2012 using a towed streamer EM acquisition system. It is a challenging target based on the fact that it is an average size oil and gas field with an average transverse resistance located at 2,100 m below mudline. Two survey lines were completed, neither one traversing the depocenter. Without data from the central part of the reservoir it was deemed appropriate to simplify the analysis by performing a fast 1D inversion for all common midpoint locations along the lines, and concatenate the results to form continuous 2D lines. Both the vertical and horizontal resistivities were inverted for by minimizing the difference in the frequency responses between forward modeled data and the acquired towed streamer EM field data. The inversions were done with only an eleven layer depth model for the overburden and reservoir, plus one extra value for the underburden. The charged reservoir shows a high anisotropy of 5, as expected for a submarine fan deposition with a high net-to-gross sequence of interbedded sands and shales. The proximal overburden shows an anisotropy of 2.6. With the vertical and horizontal resistivity and a known shale resistivity, the net-to-gross can be extracted as well as the sand resistivity. These parameters together with porosity, brine resistivity, and total charged reservoir volume estimated from seismic facilitates an estimate of the total hydrocarbon volume in place. Further, when a charged reservoir is showing strong anisotropy and it is located in proximity of, or directly on top of basement, it can be detected by means of the anisotropy alone. The basement is expected to be isotropic, or possibly display reversed anisotropy due to vertical fractures that are both more abundant and more conductive due to larger fracture aperture than the horizontal fractures.

Introduction

Conventional controlled source electro-magnetic (CSEM) marine surveys have traditionally been node-based systems with the single-station receivers emplaced on the seafloor in a very sparse line or areal configuration. The source is then towed close to the seafloor emitting a constant source signal, which is typically a square wave, where the fundamental frequency is based on what is assumed to provide optimal sensitivity to the target. The design was optimized for large water depths where the water column will absorb the so called airwave that travels up through the water from the source, laterally across in the air and down to the receivers, where it interferes with the wave of interest, namely the wave that travels through the rock column. Other arguments were that stationary receivers have much lower noise and all components of the electrical and magnetic fields can be acquired for a more uniquely constrained inversion. The high cost of data acquisition would then be offset by the need to de-risk the very costly deep water wells.

Obviously a towed acquisition system would be much more efficient and operate at a lower cost. The reason nobody has been able to develop such a system until now is that a receiver dipole that is moving in the earth's magnetic field will suffer from induced electric field noise unless it is mitigated in the hardware design. The first commercially available towed streamer EM system was tested in its final form in October 2012 in the North Sea. The similarities to 2D seismic are obvious and simultaneous acquisition of 2D seismic and EM is indeed possible. The towed streamer measures only the inline E-field, but this is actually sufficient to facilitate inversion to both vertical and horizontal resistivities in shallow waters. The towed streamer EM acquisition system offers many advantages including acquisition at 4 – 5 knots, fixed source – receiver geometry, dense common midpoint (cmp) sampling, real-time quality control, and on-board processing all the way to 1D inversion of all cmps that can then be posted as continuous 2D lines.

The Alvheim-Boa reservoir is the locally familiar Heimdal sandstone deposited as a sub-marine fan system. The reservoir shows very strong anisotropy when inverted, and this is interpreted to originate in the inter-bedded sands and shales, where the sands exhibit high resistivity due to hydrocarbon charge. With the estimated vertical and horizontal resistivities within the reservoir, together with an estimate of the shale resistivity, the resistivity of the sands can be estimated together with an estimate of the net-to-gross (N/G).

The towed streamer EM acquisition system

The layout of the acquisition system when configured for simultaneous 2D seismic is shown in Figure 1 below. The bi-pole source is 800 m long and towed at a depth of 10 m. The source runs at 1,500 A, and the source signal is user selectable. Our current favorite is the so-called Optimized Repeated Sequence (ORS). It can be viewed as a square-wave with twice the density of the discrete harmonics seen in a mono-chromatic square-wave. The signal sequence is 120 s long with the source active the first 100 s followed by 20 s of no signal that is used for background noise estimation and noise reduction processing.

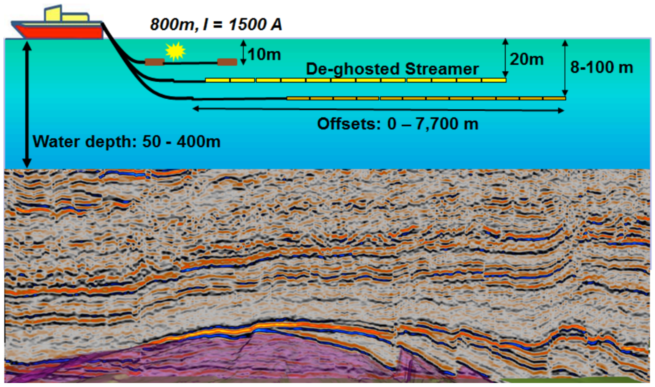

Figure 1: The layout of the acquisition system configured for simultaneous acquisition of EM and 2D seismic. The 800 m long bi-pole is towed at 10 m emitting a 1,500 A source signal. The EM streamer has offsets from 0 – 7,700 m and it is towed at a nominal depth of 100 m. The de-ghosted streamer is towed at 20 m and the towing speed is 4 – 5 knots.

The maximum nominal water depth is 400 m. Larger water depths are acceptable provided the reservoir is large, has a high transverse resistance, or is shallow below mudline.

A number of different noise reduction methods have been implemented as described by Mattsson et al (2012). Stochastic noise is attenuated in two different ways. First the dense sampling both within the streamer and along the survey lines facilitates noise reduction by stacking that improves S/N by a factor $N^{1/2}$, where N is the number of stacked signals. The second method is known as the low rank approximation based on singular value decomposition. It takes advantage of the fact that the signal only occupies discrete frequencies, whereas the stochastic noise is spread throughout the spectrum. By identifying the discrete signal frequencies, all noise between these frequencies can be removed.

The Alvheim – Boa EM data acquisition

The Alvheim-Boa reservoir was deposited as a submarine fan, and it is located at 2,100 m below mudline in 110 – 125 m water depth. The two sub-parallel survey lines strike in the NNE direction over the Boa reservoir as seen in Figure 2.

The locations of the lines is suboptimal due to permit constraints and existing infrastructure in the area, but they are traversing close to the Boa depocenter as mapped from the seismic data and seen in warm colors to the left of the survey lines shown as magenta dotted lines. Immediately to the right of the survey lines is a reference line showing the common distance for both lines from an arbitrary point outside the reservoir. The direction of sailing is also shown as south to north for Line 201 and north to south for Line 202.

Figure 3 shows the deep induction log (red) from well 24/6-1 in the field located close to 8,500 m common line location. The reservoir is not hydrocarbon charged in this location. The green curve is a shale-resistivity model based on the sonic log as described in Engelmark (2010). The yellow highlights the Utsira sand (100 – 710 m) and the Heimdal sand, which is the Alvheim – Boa reservoir (2040 – 2320 m).

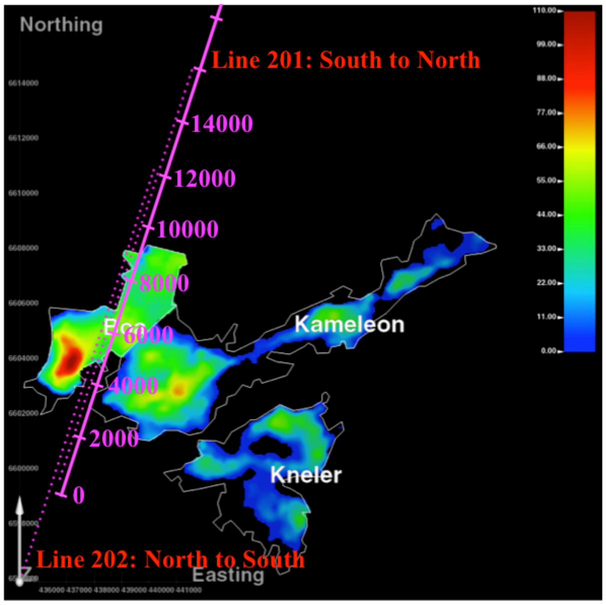

Figure 2: The Alvheim – Boa oil and gas field. The two survey lines are shown as magenta dotted lines. The Boa depocenter mapped from seismic is seen as the red anomaly immediately to the left of the lines. The color scale shows the reservoir thickness in meters. The solid magenta line is a reference line labeled in meters common to both lines.

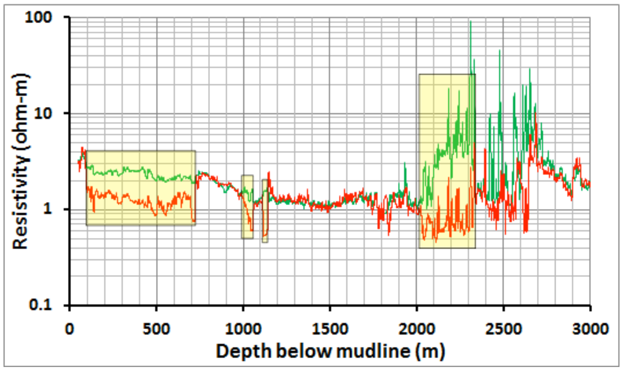

Figure 3: Deep induction resistivity log (red) from well 24/6-1 penetrating the Boa reservoir (2,020 – 2, 330 m below mudline) outside the hydrocarbon charged volume. The green curve is a shale-resistivity model based on logged velocity. Highlighted in yellow are the Utsira sand (shallow) and the Heimdal reservoir (deep) where the shale model deviates from the logged data as expected.

The shale model deviates from the logged resistivity in the sands as expected. The deep induction log shown here measures the horizontal resistivity. Modern tri-axial tools that simultaneously measure vertical and horizontal resistivity have been introduced, but are still rarely used.

Result 1: Inverting to resistivity

The vertical and horizontal resistivities below mud-line were estimated by means of 1D multi-trace anisotropic inversions for each cmp along the survey lines. The 1D inversions were then concatenated to show the resistivity as a continuous 2D profile along each line. The inversion is formulated as a minimization problem using a trust-region-reflective algorithm based on the interior-reflective algorithm described by Coleman and Li (1994, 1996). The associated frequency response uncertainties are used in the weights to down-scale the noisy data.

For both survey lines a twelve-layer model was estimated at each cmp. The bathymetry was estimated from echo sounder measurements on board the vessel and the seawater conductivity was included in the inversion. The water depth varies from 110 m in the north of the lines to 125 m in the south area. Interpreted stratigraphic surfaces in the seismic cross sections were used as constraints in the inversion of the sub-bottom resistivities. The Heimdal reservoir itself, also mapped in depth and thickness according to the well log, was then discretized into seven layers each 70 m thick followed by a half-space of under-burden. All subsurface layers thicknesses were kept fixed during the inversions, and it is only the vertical and horizontal resistivities that were inverted for.

Frequency response data at six frequencies between 0.05 and 0.75 Hz and twelve offsets ranging 1700 m to 7500 m were used for all the inversions. This data set enables sufficient sensitivity for both the vertical and horizontal resistivity from the mud-line down to 2600 m below mud-line. The minimum detectable resistivity change in each of the layers given the corresponding total uncertainty in the data is plotted in figure 4. It is clearly seen that the selected in-line data has roughly the same sensitivity for both the vertical and horizontal resistivity. The relatively thick overburden layers imply a resolution below 0.1 Ωm. The smallest possible detectable resistivity change within the thinner layers at the reservoir depth is about 1 Ωm which is sufficient to resolve the resistivity increase in the hydrocarbon filled reservoir layers.

Even though shorter offsets were recorded, they were neglected in the data going into the inversion. The reason is that a more finely resolved subsurface depth model is necessary to capture the variations that are relevant to these short offsets. However, to roughly estimate the overburden and characterize the deeper anomalous region, the offsets from 3,550 – 7,450 m are sufficient.

The relative difference, or misfit, between the measured and the modeled frequency responses after inversion were plotted as a function of offset and frequency for both the amplitude and the phase. The result for the relative difference in the amplitude shown in Figure 5 is largely below 4%. Similarly, the phase difference is seen to be below 2% in Figure 6. These values are at similar levels as the residual noise in the field data after processing, hence providing a natural lower limit in the minimization process of the measured to modeled difference.

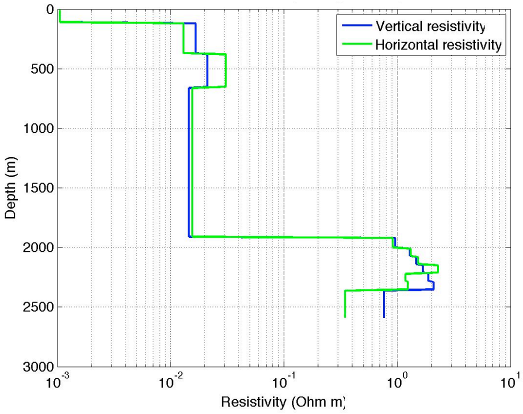

Figure 4: The resulting sensitivity with respect to vertical (blue) and horizontal (green) resistivity expressed as minimum detectable resistivity in each of the layers.

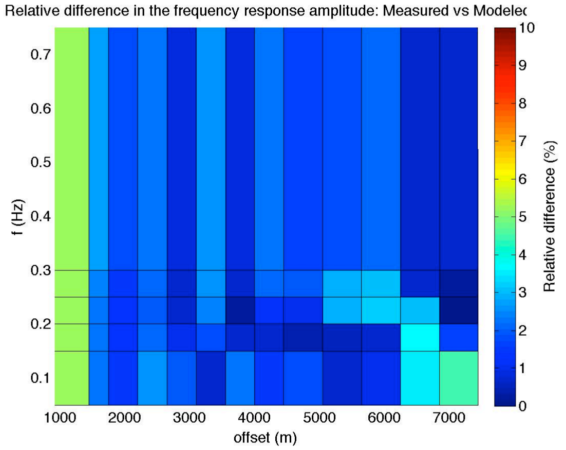

Figure 5: Example of the difference between measured and modeled frequency amplitude response.

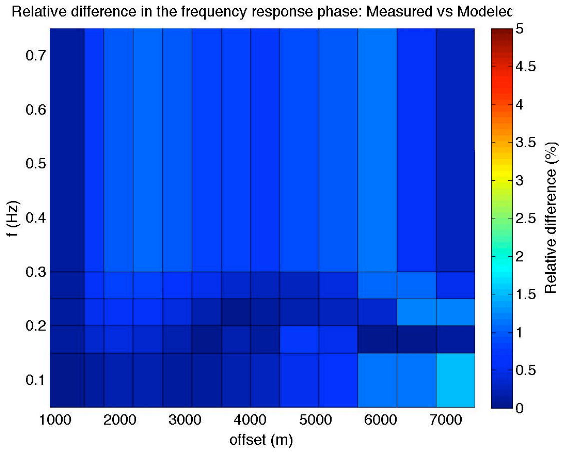

Figure 6: Example of the measured and modeled frequency phase response.

Result 2: Converting resistivity to oil & gas in place

Following the inversion, the resulting vertical and horizontal resistivity cross sections are shown in Figures 7 & 8 respectively for Line 201. Neither line traverses the depocenter but Line 201 is somewhat closer than Line 202, hence likely to be more representative. The positions of the anomalies coincide well with the maximum seismic amplitude as seen on Figure 2. The vertical resistivity rises to 50 ohm-m within the reservoir and the horizontal resistivity increases to 10 ohm-m at the same depth resulting in an anisotropy ratio of 5. Hence, even in a rather thin reservoir layer there is still some sensitivity to the horizontal component in the inline data. In comparison the anisotropy in the proximal overburden is estimated at 2.6 ohm-m.

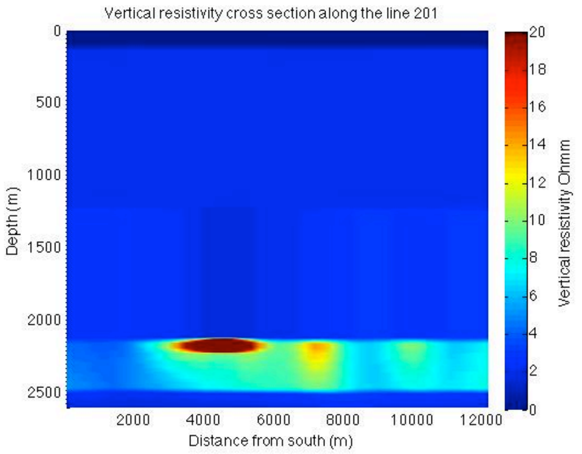

Figure 7: The estimated vertical resistivity for Line 201.

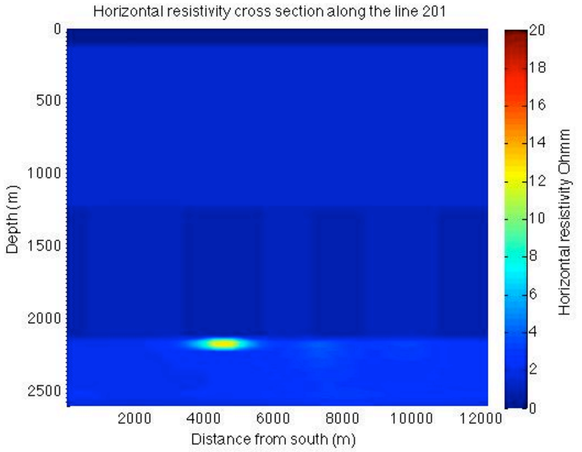

Figure 8: The estimated horizontal resistivity for Line 201.

The vertical resistivity R_v is the volumetrically weighted arithmetic average:

$$R_v = V_{sh}R_{sh} + V_{sd}R_{sd}$$

The horizontal resistivity *Rh* is the volumetrically weighted harmonic average:

$$\frac{1}{R_h} = \frac{V_{sh}}{R_{sh}} + \frac{V_{sd}}{R_{sd}}$$

where V_{sh} = shale volume; R_{sh} = shale resistivity; V_{sd} = sand volume; and R_{sd} = sand resistivity

The analysis can then be further pursued by taking three known reference data points:

- The resistivity is known for the shales within the reservoir from well logs in the area. The horizontal resistivity averages 1.1 ohm-m and with an average expected shale anisotropy of 2.0, the vertical resistivity of the shales can be expected to be ~2.2 ohm-m.
- The vertical resistivity for the charged reservoir is estimated at 50 ohm-m.
- The horizontal resistivity is estimated at 10 ohm-m.

This is sufficient information to draw up an analysis such as the one seen in Figure 9, where the straight red line represents the vertical resistivity as a function of N/G, and the blue line at the bottom with the dramatic rise to the right represents the horizontal resistivity as a function of N/G.

The known points are the vertical and horizontal anisotropic shale resistivity (2.2 & 1.1 ohm-m) to the lower left highlighted in green. The vertical resistivity for the whole charged reservoir is known to be 50 ohm-m, and the corresponding horizontal resistivity, which is estimated at 10 ohm-m. This will then uniquely determine the N/G which is found to be 0.91 where the vertical and horizontal resistivities are found, and the sand resistivity is also uniquely determined at 55 ohm-m highlighted in yellow to the upper right.

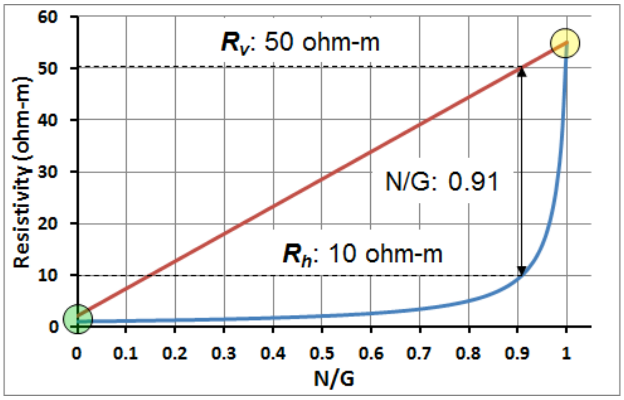

Figure 9: The red and blue lines are the vertical and horizontal resistivity, respectively, as a function of N/G. Three points are known: the anisotropic shale resistivities (2.2 & 1.1 ohm-m) to the lower left circled in green, and the vertical and horizontal resistivities for the reservoir at 50 and 10 ohm-m respectively. This allows us to estimate N/G at 0.91 and the resistivity of the sands at 55 ohm-m.

All the information is now available to estimate the total hydrocarbon volume in place:

- Sand resistivity and N/G from the inversion.

- Sand porosity and brine resistivity (R_w) from well logs. If there are no wells in the area, the porosity can be estimated from inverted seismic data. R_w can be estimated based on an assumed salinity of seawater and an estimated temperature gradient.
- Total charged reservoir volume from depth converted seismic data.

With the sand resistivity, the sand porosity and R_w from the well logs, it is now possible to estimate the water saturation, and hence also the hydrocarbon saturation in the sands based on the Archie equation. By incorporating the N/G and the total charged reservoir volume from the depth converted seismic, it is then possible to estimate the total hydrocarbon volumes in place.

The ability to evaluate both vertical and horizontal resistivity is also very important when evaluating a reservoir in the vicinity of, or directly on top of, a high resistivity basement or other resistive body. This has traditionally been considered a difficult problem to resolve. However, assuming the basement is either isotropic, or displays inverse anisotropy where the horizontal resistivity is larger than the vertical, as would be the case if the basement is fractured. Vertical fractures are expected to be more frequent and with a wider aperture facilitating better conductivity than the horizontal fractures. Hence, if the charged reservoir shows strong anisotropy, then it can be uniquely identified based on the anisotropy alone.

Conclusions

The Alvheim – Boa reservoir is a challenging target due to the combination of depth below mudline (2,100 m), limited lateral extension (2,000 m) and a low to average transverse resistance of the charged reservoir. An additional weakness is the suboptimal positioning of the survey lines that traverse off the side of the depocenter, further reducing the signal and adding uncertainty. Due to the lack of data from the central part of the charged reservoir, it was decided to avoid 2 ½ D inversion. Instead, as a proof of concept, a series of fast 1D inversions were concatenated to form continuous 2D lines, facilitating an estimate of maximum vertical and horizontal resistivity in the reservoir. The vertical and horizontal resistivity together with an estimated shale resistivity facilitates an evaluation of charged sand resistivity and N/G. With porosity and brine resistivity estimated in the wells, the hydrocarbon saturation can be estimated based on Archie's equation, and with the total charged reservoir volume mapped from depth converted seismic, the total hydrocarbon volumes in place can then be estimated.

In addition, the fact that vertical and horizontal resistivity can be estimated from the towed streamer EM data facilitates detection of a strongly anisotropic reservoir even when it is located immediately on top of basement. The basement will be isotropic, or possibly show reversed anisotropy based on the more frequent vertical fractures. In such a situation, the reservoir can be confidently detected based on anisotropy alone.

Acknowledgments

The authors are grateful to PGS for allowing us to publish the data.

References

T F Coleman and Li Y, An Interior, Trust Region Approach for Nonlinear Minimization Subject to Bounds, SIAM Journal on Optimization, Vol. 6, pp. 418–445, 1996.

T F Coleman and Li Y, On the Convergence of Reflective Newton Methods for Large-Scale Nonlinear Minimization Subject to Bounds, Mathematical Programming, Vol. 67, Number 2, pp. 189–224, 1994.

Folke Engelmark: Velocity to resistivity transform via porosity, SEG Technical Program Expanded Abstracts 2010.

Johan Mattsson, Peter Lindqvist, Robert Juhasz, and Erik Björnemo, Noise reduction and error analysis for a Towed EM System, SEG Technical Program Expanded Abstracts 2012: 1-5.